Applied Mathematical Modelling 000 (2016) 1–17

Contents lists available at ScienceDirect

Applied Mathematical Modelling

journal homepage: www.elsevier.com/locate/apm

The point-to-point multi-region energy-saving trajectory planning for a mechatronic elevator system

Kun-Yung Chen[a], Rong-Fong Fung[b,*]

[a] Department of Mechanical Engineering, Air Force Institute of Technology, No. 198, Jieshou W. Rd., Gangshan Dist., Kaohsiung City 820, Taiwan

[b] Department of Mechanical and Automation Engineering, National Kaohsiung First University of Science and Technology, No. 1, University Rd., Yanchao Dist., Kaohsiung City 824, Taiwan

ARTICLE INFO

Article history:
Received 15 April 2015
Revised 1 April 2016
Accepted 7 June 2016
Available online xxx

Keywords:
Constraint condition
Input absolute electrical energy (IAEE)
Mechatronic system
Self-learning particle swarm optimization (SLPSO)

ABSTRACT

A mechatronic elevator system driven by a permanent magnet synchronous motor (PMSM) is completely modeled by the mechanical and electrical equations. The electrical energy equation, including input, dissipation, magnetic and kinetic energies, is formulated for energetic analysis. The adjusting fraction, defined as the flight time from null to maximum acceleration with respect to the total acceleration time, is optimized by the self-learning particle swarm optimization (SLPSO) method in minimizing the input absolute electrical energy (IAEE). In this paper, multi-region trajectories of high-degree polynomials with constraints of maximum acceleration and velocity are planned, and the flight time and the IAEE are compared numerically. The main contribution of this paper is to propose a methodology in the point-to-point (PTP) multi-region energy-saving trajectory planning for any mechatronic system.

1. Introduction

The energy consumption is a popular topic and enthusiastically discussed by researchers and engineers nowadays. Human seriously consumes the energy in variable systems. How to save energy is the significant and emergent issue in our life. Therefore, energy saving is an importantly practicable stratagem for any system. In this paper, the trajectory planning and energy analysis will be discussed and investigated in a point-to-point (PTP) motion profile of a mechatronic elevator system. In the previous paper [1] about trajectory planning, the problem of minimum-time trajectory planning was studied for a three degree-of-freedom planar manipulator using a hierarchical hybrid neuro-fuzzy system. The use of finite impulse response filters for planning minimum-time trajectories for robots or automatic machines under constraints of velocity, acceleration, etc. was also presented and discussed [2]. An optimization approach [3] was proposed to generate smooth and time-optimal constrained tool trajectories for Cartesian computer numerical control manufacturing systems. A high smooth trajectory, planning method [4] was designed by a combination of the planning with multi-degree splines in Cartesian space and multi-degree B-spline in a joint space. A hybrid algorithm combining the particle swarm optimization (PSO) algorithm with Legendre pseudo-spectral method [5], was proposed for solving time-optimal trajectory planning problems of under-actuated spacecrafts. Trajectory planning was considered by Lambrechts et al. [6] with given constraints and a feedforward

* Corresponding author. Tel.: +886 936659758; fax: +886 7 6011066.
E-mail addresses: chenkunyung@yahoo.com.tw (K.-Y. Chen), rffung@nkfust.edu.tw (R.-F. Fung).

http://dx.doi.org/10.1016/j.apm.2016.06.001
0307-904X/

controller for single-axis motion control. In the previous papers [1–6], the authors emphasized the optimal-time trajectory planning, but large energies were also consumed in the operation process.

The resulting trajectory was required smooth enough, and an objective function containing a term proportional to the integral of squared jerk along the trajectory was considered in [7], where the fifth-order and B-spline trajectories were used to compose of the overall trajectory. A real-time interpolation algorithm for trajectory planning was studied by Wang et al. [8], where the non-uniform rational basis spline interpolation algorithm was proposed to confine the contour errors and feedrate fluctuations. In planning the linear and circular arc trajectories [9], the robot starts its motion from a start point with zero velocity to the end point on the desired trajectory and stops at the end point. The manipulator trajectory using algebraic-trigonometric Hermite polynomials curves [10] was designed to interpolate data points for the manipulator via given curves. The optimal jerk-limited PTP trajectories for flexible-link robotic manipulators were developed in [11]. On-line smooth trajectory generation for industrial mechatronic systems was addressed in [12]. An optimal trajectory planning technique for suppressing residual vibrations in two-link rigid-flexible manipulators was proposed by Abe [13]. The typical bilateral force constraints of the cables were translated into the velocity and acceleration of the cable-direct-driven-robot end-effecter along the path by Trevisani [14]. The constraints were computed by use of the robot dynamic model, and then incorporated into a suitable trajectory planning algorithm to yield the minimum traversal time.

From the review of the above studies [1–14], the energy consumption was not considered in the trajectory planning for systems' models. On the other hand, [15–19] considered the systems with energy-saving thought, and can be depicted more clearly as follows. A nonlinear constrained optimal control problem [15] was originated from the optimal trajectory planning of servomotor systems. It is noted that the quadratic cost function in [15] is a Hamiltonian function, but not the definition of physical energy for servomotor systems. The manipulator trajectories [16] were modeled by using a parametric path representation, and the optimal trajectory was then obtained by using a hybrid scheme comprising the particle swarm optimization method and the local conjugate gradient method. The PTP trajectory [17–19] was described by a high-degree polynomial, which satisfies the end conditions of displacement, velocity, acceleration and jerk at the initial and final times. The real-coded genetic algorithm method was employed to determine the polynomial coefficients by minimizing the input electrical energy. However, under some constraint conditions (for examples, constraints on the velocity, acceleration or jerk), the proposed method was difficult to find the optimal coefficients of the high-degree polynomials, which satisfy the fitness function and constraint conditions simultaneously.

To obtain both the performances satisfying the minimum input electrical energy and constraint conditions for the trajectory planning, this paper proposed the method of multi-region trajectory planning. Firstly, the modeling of the elevator system is formulated, and the system's electrical energy equation is found. Secondly, the car's maximum velocity, acceleration and final position are specified. A seven-region (7-R) trajectory [20] with five-degree (5-D) polynomial is compared with our proposed method in finding the minimum input absolute electrical energy (IAEE) trajectory. Thirdly, the self-learning particle swarm optimizer (SLPSO) [21,22] is implemented to find the optimal value of the fraction, defined as the flight time from null to maximum acceleration with respect to the total acceleration time, by minimizing the IAEE. It is also found that non-maximum acceleration flight time has the minimum IAEE. Therefore, a 7-R trajectory is substituted for the 5-R to obtain the minimum IAEE trajectory. It can be concluded that when the trajectory has a large input energy, it also has a short flight time. On the contrary, when the trajectory has a small IAEE, then has a large flight time. Fourthly, to simplify the trajectory planning of a 5-R trajectory, a 3-R trajectory with 7-D polynomial trajectory is proposed under the same constraint conditions. The fraction is undetermined, and can also be searched by the SLPSO by minimizing the IAEE. Finally, the 5- and 3-R trajectories are compared in the IAEE and flight time, and it is summarized that the IAEE and flight time are contradictory in the PTP trajectory planning.

2. Modeling of the elevator system

In this section, the equations of the mechatronic elevator system are to be formulated. The complete energy equations including the electrical and mechanical systems are formulated from the physical model.

2.1. Dynamic equations of the mechatronic system

To analyze and investigate the mechatronic system, it is important to formulate the dynamic modeling. The mechatronic elevator system consists of the permanent magnet synchronous motor (PMSM) and elevator mechanism. Fig. 1(a) shows the physical model of the mechatronic elevator system, where T_c and T_w are the tensions in the car and counterweight sides, respectively. The main cable passing over the drive sheave is attached to the car and counterweight. T_l is the torque applied on the reducer, θ and ω are respectively the angular displacement and velocity of the sheave, R is the radius of the sheave, H is the length between the original position and sheave center point, x_{c0} and x_{w0} are the initial positions of the car and counterweight, respectively, m_c, Δm_c and m_w are the car's, passengers' and counterweight's masses, respectively. x_c, v_c, and a_c are the car's displacement, velocity and acceleration, respectively. x_w, v_w, and a_w are the counterweight's displacement, velocity and acceleration, respectively. Fig. 1(b) shows the control block diagram of the elevator system driven by a PMSM. According to the dynamic equation of the elevator mechatronic system [23], the mechanical and electrical equations can be found as follows:

$$\dot{\theta} = \omega, \tag{1a}$$

Please cite this article as: K.-Y. Chen, R.-F. Fung, The point-to-point multi-region energy-saving trajectory planning for a mechatronic elevator system, Applied Mathematical Modelling (2016), http://dx.doi.org/10.1016/j.apm.2016.06.001

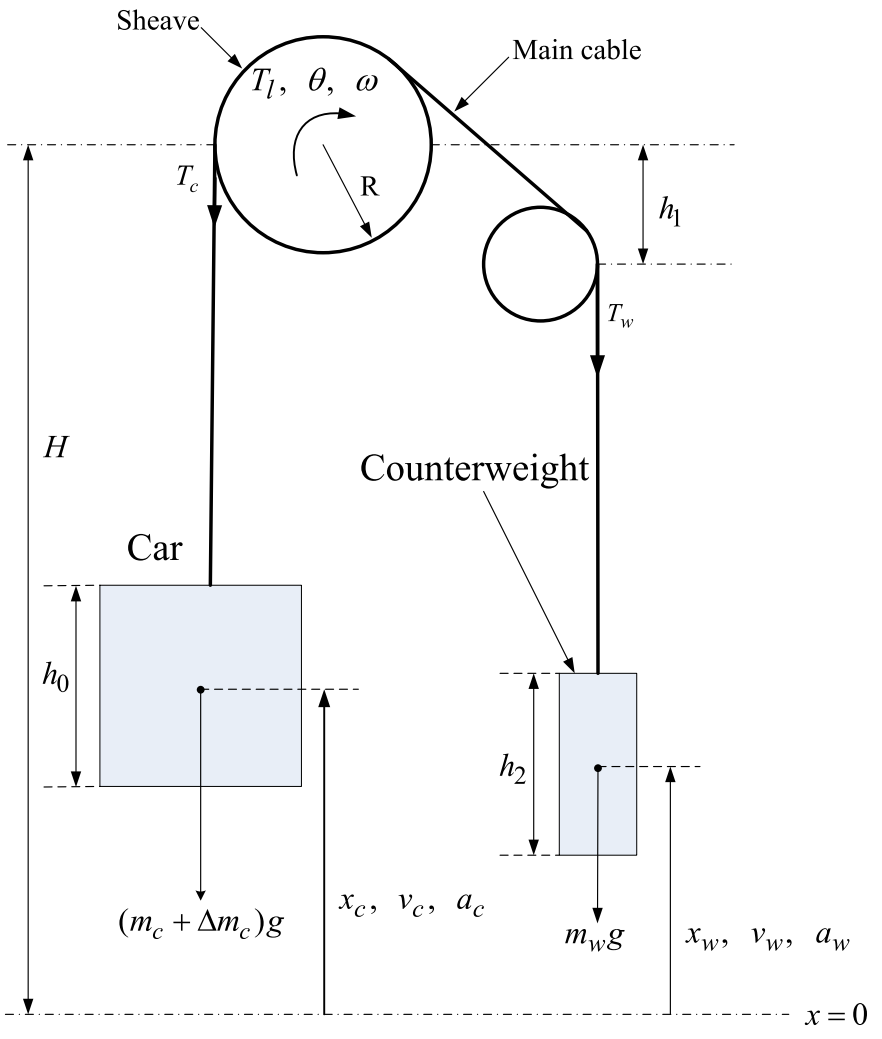

Fig. 1. Elevator mechatronic system driven by a PMSM: (a) physical model, (b) PMSM drive system.

$$(J_t + \Delta J)\dot{\omega} = 2\rho g R^2 \theta - (n^2 B_m + cR^2)\omega + nK_t i_q + \Delta d, \tag{1b}$$

$$v_q = R_s i_q + L_q \frac{d}{dt} i_q + \lambda_d n\omega, \tag{1c}$$

where $J_t = J + n^2 J_m + m_c R^2 + m_w R^2 + [2H - (\frac{h_0}{2} + h_1 + \frac{h_2}{2}) - (x_{c0} + x_{w0})]\rho R^2$, $\Delta J = \Delta m_c R^2$ and $\Delta d = [(\frac{h_0}{2} + x_{c0} - h_1 - \frac{h_2}{2} - x_{w0})\rho + (m_w - m_c - \Delta m_c)]gR$.

Please cite this article as: K.-Y. Chen, R.-F. Fung, The point-to-point multi-region energy-saving trajectory planning for a mechatronic elevator system, Applied Mathematical Modelling (2016), http://dx.doi.org/10.1016/j.apm.2016.06.001

It is noted that ΔJ is the uncertain rotational inertia, Δd is the uncertain torque due to cable and passengers' masses, c is the viscous coefficient of the car's guide and v_q is the control input voltage. Therefore, the state-space matrix of the mechatronic elevator system, Eqs. (1a)–(1c) can be written as follows:

$$\dot{\mathbf{X}} = \mathbf{A}\mathbf{X} + \mathbf{B}u + \mathbf{Q}, \tag{2}$$

where $\mathbf{X} = [\theta \quad \omega \quad i_q]^T$, $\mathbf{A} = \begin{bmatrix} 0 & 1 & 0 \\ \frac{2\rho g R^2}{J_t+\Delta J} & \frac{-(n^2B_m+cR^2)}{J_t+\Delta J} & \frac{nK_t}{J_t+\Delta J} \\ 0 & \frac{-n\lambda_d}{L_q} & \frac{-R_s}{L_q} \end{bmatrix}$, $\mathbf{B} = \begin{bmatrix} 0 & 0 & \frac{1}{L_q} \end{bmatrix}^T$, $\mathbf{Q} = \begin{bmatrix} 0 & \frac{\Delta d}{J_t+\Delta J} & 0 \end{bmatrix}^T$ and $u = v_q$.

2.2. Energy equations

It is interesting to find the energy equations of the mechatronic system, which includes electrical and mechanical parts. In the dynamical equations in Eqs. (1b) and (1c), multiplying i_q to Eq. (1c) and integrating with respect to time to the final time T, the electrical energy can be found as follows:

$$\int_0^T i_q v_q dt = \int_0^T R_s i_q^2 dt + \int_0^T i_q L_q \frac{di_q}{dt} dt + \int_0^T n i_q \lambda_d \omega dt. \tag{3}$$

The item ni_q in Eq. (1b) can be found as follows:

$$ni_q = \frac{(J_t + \Delta J)}{K_t}\dot{\omega} - \frac{2\rho g R^2}{K_t}\theta + \frac{(n^2 B_m + cR^2)}{K_t}\omega - \frac{\Delta d}{K_t}. \tag{4}$$

Substituting Eq. (4) into the last term $\int_0^T ni_q\lambda_d\omega dt$ of Eq. (3), it can be found as follows:

$$\int_0^T i_q v_q dt = \int_0^T \left\{ R_s i_q^2 + \frac{\lambda_d}{K_t}[(n^2B_m + cR^2)\omega^2 - \Delta d\omega - 2\rho g R^2 \theta\omega] \right\} dt + \int_0^T i_q L_q \frac{di_q}{dt} dt + \int_0^T \frac{\lambda_d}{K_t}(J_t + \Delta J)\omega\dot{\omega} dt. \tag{5a}$$

Therefore, the energy equations of the mechatronic elevator system can be rewritten as follows:

$$E_i = E_d + E_m + E_k, \tag{5b}$$

where $E_i = \int_0^T i_q v_q dt$ is the input electrical energy, $E_d = \int_0^T \{R_s i_q^2 + (\lambda_d/K_t)[(n^2B_m + cR^2)\omega^2 - \Delta d\omega - 2\rho g R^2\theta\omega]\}dt$ is the dissipation energy, $E_m = \int_0^T i_q L_q \frac{di_q}{dt} dt$ is the magnetic energy, and $E_k = (\lambda_d/K_t)\int_0^T (J_t + \Delta J)\omega\dot{\omega} dt$ is the kinetic energy. Finally, the IAEE can be defined as

$$|E_i| = \int_0^T |i_q v_q| dt. \tag{6}$$

3. Design energy-saving trajectory with constraints

In the general trajectory design for a PTP profile, it usually requires the constraints at initial- and final-time conditions (for examples, initial and final velocities, accelerations and jerks). The maximum velocity or acceleration of the trajectories are seldom restricted. In this section, the maximum velocity, acceleration and final position are specified in the PTP multi-region trajectory profile. The 3- and 7-R movement profiles are investigated as follows.

3.1. A 7-R movement profile

In designing the trajectory, the car's maximum velocity $v_{\max}$, maximum acceleration $a_{\max}$ and the final position h are specified and given. The acceleration function of the car is divided into seven regions [20] and is shown in Fig. 2(a). The detailed equations of the displacement, velocity, acceleration and jerk in these regions by using a 5-D polynomial trajectory can be written as follows:

$$x_i(t) = b_{i0} + b_{i1}(t - t_{i-1}) + b_{i2}(t - t_{i-1})^2 + b_{i3}(t - t_{i-1})^3 + b_{i4}(t - t_{i-1})^4 + b_{i5}(t - t_{i-1})^5, \tag{7a}$$

$$v_i(t) = b_{i1} + 2b_{i2}(t - t_{i-1}) + 3b_{i3}(t - t_{i-1})^2 + 4b_{i4}(t - t_{i-1})^3 + 5b_{i5}(t - t_{i-1})^4, \tag{7b}$$

$$a_i(t) = 2b_{i2} + 6b_{i3}(t - t_{i-1}) + 12b_{i4}(t - t_{i-1})^2 + 20b_{i5}(t - t_{i-1})^3, \tag{7c}$$

$$j_i(t) = 6b_{i3} + 24b_{i4}(t - t_{i-1}) + 60b_{i5}(t - t_{i-1})^2. \tag{7d}$$

where i ($i = 1,2, \ldots, 7$) is the region number, b_{in} ($n = 1,\ldots, 5$) are the unknown coefficients and can be determined by the initial and final conditions, t_{i-1} is the initial time in region i. For simplicity, the durations of regions 1, 3, 5 and 7 are set to be the same. Here, a fraction σ of the total acceleration (t_0 to t_3) or deceleration (t_4 to t_7) time is defined as follows:

$$t_1 - t_0 = t_3 - t_2 = t_5 - t_4 = t_7 - t_6 = \sigma(t_3 - t_0) = \sigma(t_7 - t_4), \quad 0 \le \sigma \le 0.5. \tag{8}$$

Please cite this article as: K.-Y. Chen, R.-F. Fung, The point-to-point multi-region energy-saving trajectory planning for a mechatronic elevator system, Applied Mathematical Modelling (2016), http://dx.doi.org/10.1016/j.apm.2016.06.001

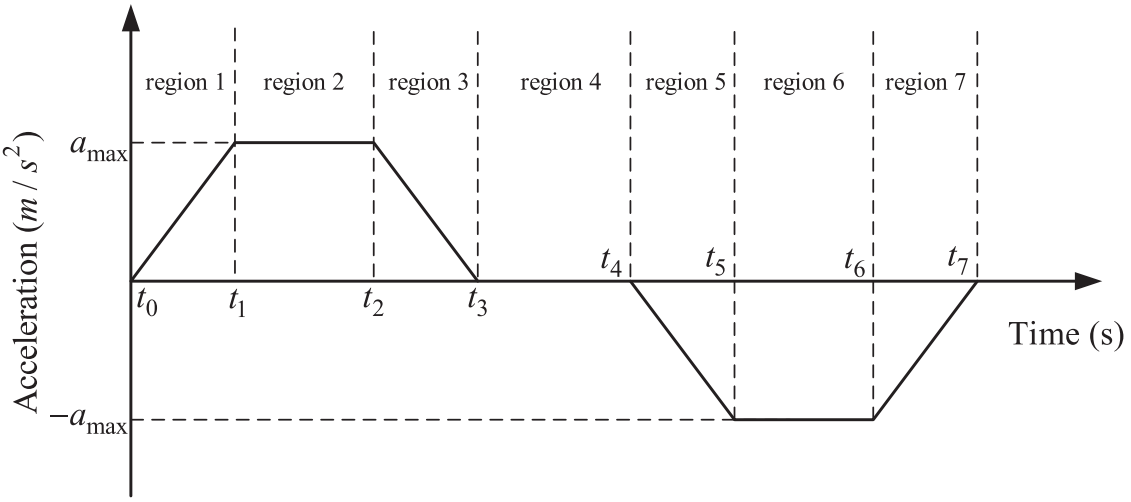

(a) A 7-R acceleration profile

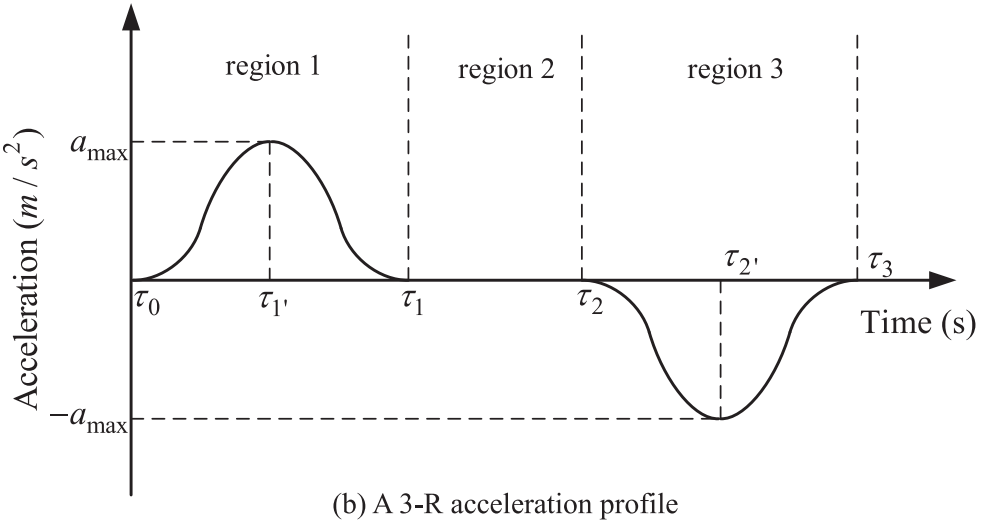

(b) A 3-R acceleration profile

Fig. 2. Acceleration profile with (a) 7-R and (b) 3-R.

By adjusting the fraction σ, the time in maximum acceleration and maximum deceleration can be found. For example, $\sigma = 0$, there are no regions 1, 3, 5 and 7, and the infinite jerk happens at time t_0 and t_7. But the case $\sigma = 0$ has the shortest flight time. When $\sigma = 0.5$, it has no duration for maximum acceleration and maximum deceleration, regions 2 and 6 become a point, and the case results the longest flight time. The detailed displacement, velocity, acceleration and jerk equations in every region can refer to [20].

3.2. A 3-R movement profile

In the 3-R moving profile, the car's maximum velocity v_{max}, maximum acceleration a_{max} and the final position h are also given and specified. The acceleration function of the car is divided into three regions in Fig. 2(b), which is acceleration, constant velocity and deceleration. The acceleration region is from τ_0 to τ_1 and maximum acceleration is specified at time $\tau_{1'}$. Constant velocity region is from time τ_1 to τ_2. The deceleration region is from time τ_2 to τ_3 and maximum deceleration is specified at time $\tau_{2'}$. For simplicity, the acceleration and deceleration regions have the same flight time ($\tau_3 - \tau_2 = \tau_1 - \tau_0$). In the acceleration and deceleration regions, a 7-D polynomial trajectory is applied and the details of the displacement, velocity, acceleration and jerk are written as follows:

$$x_i(\tau) = c_{i0} + c_{i1}(\tau - \tau_{i-1}) + c_{i2}(\tau - \tau_{i-1})^2 + c_{i3}(\tau - \tau_{i-1})^3 + c_{i4}(\tau - \tau_{i-1})^4 + c_{i5}(\tau - \tau_{i-1})^5 + c_{i6}(\tau - \tau_{i-1})^6 + c_{i7}(\tau - \tau_{i-1})^7, \quad (9a)$$

Please cite this article as: K.-Y. Chen, R.-F. Fung, The point-to-point multi-region energy-saving trajectory planning for a mechatronic elevator system, Applied Mathematical Modelling (2016), http://dx.doi.org/10.1016/j.apm.2016.06.001

$$v_i(\tau) = c_{i1} + 2c_{i2}(\tau - \tau_{i-1}) + 3c_{i3}(\tau - \tau_{i-1})^2 + c_{i4}(\tau - \tau_{i-1})^3 + 5c_{i5}(\tau - \tau_{i-1})^4 + 6c_{i6}(\tau - \tau_{i-1})^5 + 7c_{i7}(\tau - \tau_{i-1})^6, \tag{9b}$$

$$a_i(\tau) = 2c_{i2} + 6c_{i3}(\tau - \tau_{i-1}) + 12c_{i4}(\tau - \tau_{i-1})^2 + 20c_{i5}(\tau - \tau_{i-1})^3 + 30c_{i6}(\tau - \tau_{i-1})^4 + 42c_{i7}(\tau - \tau_{i-1})^5, \tag{9c}$$

$$j_i(\tau) = 6c_{i3} + 24c_{i4}(\tau - \tau_{i-1}) + 60c_{i5}(\tau - \tau_{i-1})^2 + 120c_{i6}(\tau - \tau_{i-1})^3 + 210c_{i7}(\tau - \tau_{i-1})^4. \tag{9d}$$

where i ($i = 1, 2, 3$) is the region number, c_{in} ($n = 1,\ldots, 7$) are the unknown coefficients and are determined by the initial and final conditions. τ_{i-1} is the initial time in region i. The duration of regions 1 and 3 are set to be a fraction η of the time with respect to the total acceleration (τ_0 to τ_1) or deceleration (τ_2 to τ_3) time as follows:

$$\eta = \frac{\tau_{1'} - \tau_0}{T_1} = \frac{\tau_3 - \tau_{2'}}{T_1}, \quad \text{where} \quad 0 < \eta < 1 \quad \text{and} \quad T_1 = \tau_1 - \tau_0 = \tau_3 - \tau_2. \tag{10}$$

By adjusting the fraction η, the times reaching to the maximum acceleration and deceleration at regions 1 and 3 can be found, respectively. The trajectories of the three regions by a 7-D polynomial are described as follows.

(1) Region 1 trajectory

The coefficients of region 1 trajectory are determined by the initial and final constraint conditions, which are described as

$$x_1(\tau_0) = 0, \quad v_1(\tau_0) = 0, \quad v_1(\tau_1) = v_{\max}, \quad a_1(\tau_0) = 0, \quad a_1(\tau_1) = 0, \quad a_1(\tau_{1'}) = a_{\max},$$
$$j_1(\tau_0) = 0, \quad j_1(\tau_1) = 0 \quad \text{and} \quad j_1(\tau_{1'}) = 0. \tag{11a–i}$$

From the above 11 constraint conditions in Eq. (11a–i), the unknown coefficients $c_{10}, c_{11}\ldots, c_{17}$ and T_1 can be found as

$$c_{10} = c_{11} = c_{12} = c_{13} = 0, \qquad c_{14} = \frac{(5\eta - 3)(1 - 5\eta + 5\eta^2)^2 a_{\max}^3}{10800(-1+\eta)^9 \eta^8 v_{\max}^2},$$
$$c_{15} = -\frac{(1 - 5\eta + 5\eta^2)^3(-1 - \eta + 5\eta^2)a_{\max}^4}{270000(-1+\eta)^{12}\eta^{12}v_{\max}^3}, \quad c_{16} = \frac{(1 - 5\eta + 5\eta^2)^4(-4 + 5\eta + 5\eta^2)a_{\max}^5}{24300000(-1+\eta)^{15}\eta^{15}v_{\max}^4},$$
$$c_{17} = -\frac{(2\eta - 1)(1 - 5\eta + 5\eta^2)^5 a_{\max}^6}{510300000(-1+\eta)^{18}\eta^{18}v_{\max}^5} \quad \text{and} \quad T_1 = \frac{30(\eta - 1)^3\eta^3 v_{\max}}{(1 - 5\eta + 5\eta^2)a_{\max}}. \tag{12a–f}$$

(2) Region 2 trajectory

Region 2 trajectory has the constant velocity and is described as follows.

$$x_2(\tau) = x_1(\tau_1) + v_{\max}(\tau - \tau_1), \quad v_2(\tau) = v_{\max} \quad \text{and} \quad a_2(\tau) = j_2(\tau) = 0. \tag{13a–c}$$

(3) Region 3 trajectory

The coefficients of region 3 trajectory are determined by the initial and final constraint conditions, which are described as

$$x_3(\tau_3) = h, \quad v_3(\tau_2) = v_{\max}, \quad v_3(\tau_3) = 0, \quad a_3(\tau_2) = 0, \quad a_3(\tau_3) = 0,$$
$$a_3(\tau_{2'}) = -a_{\max}, \quad j_3(\tau_2) = 0, \quad j_3(\tau_3) = 0 \quad \text{and} \quad j_1(\tau_{2'}) = 0. \tag{14a–i}$$

From the above 9 boundary conditions in Eq. (14a–i), the unknown coefficients $c_{30}, c_{31}\ldots, c_{37}$ can be found as

$$c_{31} = v_{\max}, \quad c_{32} = c_{33} = 0, \quad c_{30} = \frac{7(1 - 5\eta + 5\eta^2)^2 a_{\max} h - 15(-1+\eta)^3\eta^3(6 - 33\eta + 35\eta^2)v_{\max}^2}{7(1 - 5\eta + 5\eta^2)^2 a_{\max}},$$
$$c_{34} = -\frac{(5\eta - 2)(1 - 5\eta + 5\eta^2)^2 a_{\max}^3}{10800(-1+\eta)^8\eta^9 v_{\max}^2}, \quad c_{35} = \frac{(1 - 5\eta + 5\eta^2)^3(3 - 9\eta + 5\eta^2)a_{\max}^4}{270000(-1+\eta)^{12}\eta^{12}v_{\max}^3},$$
$$c_{36} = -\frac{(1 - 5\eta + 5\eta^2)^4(6 - 5\eta + 5\eta^2)a_{\max}^5}{24300000(-1+\eta)^{15}\eta^{15}v_{\max}^4} \quad \text{and} \quad c_{37} = c_{17}. \tag{15a–g}$$

3.3. The SLPSO

In 1995, Kennedy and Eberhart [24,25] first introduced the PSO method, which is derived from the social-psychological theory, and has been found to be robust in complex systems. But it can't be guaranteed that the PSO method can find the global coefficients to minimize the IAEE. In this paper, the SLPSO method is employed to determine the fractions σ and η. The SLPSO method has four velocity update strategies including exploitation, jumping out, exploration and convergence are described as follows

$$\text{exploitation:} \quad v_j^{(t+1)} = wv_j^{(t)} + k_1 \cdot \text{rand1} \cdot (pbest_j - x_j^{(t)}), \tag{16a}$$

Please cite this article as: K.-Y. Chen, R.-F. Fung, The point-to-point multi-region energy-saving trajectory planning for a mechatronic elevator system, Applied Mathematical Modelling (2016), http://dx.doi.org/10.1016/j.apm.2016.06.001

$$\text{jumpingout:} \quad v_j^{(t+1)} = v_j^{(t)} + v_{avg}^{(t)} \cdot N(0,1), \tag{16b}$$

$$\text{exploration:} \quad v_j^{(t+1)} = wv_j^{(t)} + k_2 \cdot \text{rand2} \cdot (pbest_{rand}^{(t)} - x_j^{(t)}), \tag{16c}$$

$$\text{convergence:} \quad v_j^{(t+1)} = wv_j^{(t)} + k_3 \cdot \text{rand3} \cdot (abest^{(t)} - x_j^{(t)}). \tag{16d}$$

where t is the pointer of iterations, $v_j^{(t)}$ is the velocity of the particle j at iteration t, w is the inertia weighting factor, k_1, k_2 and k_3 are the acceleration constants. The *rand1, rand2* and *rand3* are the random numbers between 0 to 1. The $pbest_j$ is the *pbest* of particle j so far. $x_j^{(t)}$ is the is the current position of particle j and $v_{avg}^{(t)}$ is the average velocity of all particles at iteration. $N(0, 1)$ is a random number generated from the normal distribution with mean 0 and variance 1. The $pbest_{rand}^{(t)}$ is the *pbest* of a random particle, that is better than $pbest_j$. The $abest^{(t)}$ is the archive of the best position searched by SLPSO so far. In the SLPSO, each particle has its own velocity update strategy to deal with the different situation in the real system. An adaptive learning framework at the individual level, which can enable a particle to choose the optimal strategy according to its own local fitness value, implements the cooperation of the four velocity update strategies. The detail process and performance of the SLPSO can refer to [21,22].

In this paper, the IAEE is assigned as the fitness function (F_f), which is described as follows:

$$F_f = \int_0^T |i_q v_q| dt. \tag{17}$$

Assuming the uncertainties ΔJ and Δd are null in the trajectory design. The SLPSO method is employed to find the fractions σ and η to minimize the F_f. The car's displacement, velocity, acceleration and jerk are x_c, v_c, a_c and j_c, respectively. The sheave rotation angular displacement, velocity, acceleration and jerk are θ, ω, α and j, respectively. The relationships among them can be written as follows:

$$x_c = R\theta, \quad v_c = R\omega, \quad a_c = R\alpha \quad \text{and} \quad j_c = Rj. \tag{18a–d}$$

Eq. (18a–d) are substituted into Eq. (1b) and the current i_q and its time derivative di_q/dt can be found as follows:

$$i_q = \frac{1}{nK_t}\left[J_t \frac{a_c}{R} + (n^2 B_m + cR^2)\frac{v_c}{R} - 2\rho g R x_c\right], \tag{19a}$$

$$\frac{di_q}{dt} = \frac{1}{nK_t}\left[J_t \frac{j_c}{R} + (n^2 B_m + cR^2)\frac{a_c}{R} - 2\rho g R v_c\right]. \tag{19b}$$

Therefore, the input voltage v_q of Eq. (1c) can be found by i_q, di_q/dt and v_c. Finally, the SLPSO algorithm can be used to search for proper values of σ, η and the profiles x_c, v_c, a_c and j_c, which minimize the fitness function F_f. Finally, the flow chart of the energy-saving trajectory planning by SLPSO method is illustrated in Fig. 3.

4. Numerical simulations

The constraint conditions in numerical simulations are given as: the length of the elevator movement is $h = 150m$, the car's maximum velocity is $v_{\max} = 5\ m/s$, and the maximum acceleration is $a_{\max} = 0.75\ m/s^2$. The car's initial displacement, velocity, acceleration and jerk are all null, the final displacement, velocity, acceleration and jerk are $x_c(T) = 150m$, $v_c(T) = 0m/s, a_c(T) = 0m/s^2$ and $j_c(T) = 0m/s^3$ at the final time T. The numerical simulation parameters (Group 1) performed for the elevator system model are shown as follows:

$J_m = 8 \times 10^{-4}\ kgm^2,\ B_m = 10^{-3}\ Nms/rad,\ K_t = 2\ Nm/A,\ R_s = 5\ \Omega,\ \lambda_d = 0.05\ N - s/rad,$
$L_q = 10^{-2}\ H,\ J = 0.1\ kgm^2,\ R = 0.25\ m,\ m_c = 50\ kg,\ m_w = 50\ kg,\ c = 0.5\ Ns/m,\ n = 1,$
$H = 200\ m,\ h_0 = 2\ m,\ h_1 = 1\ m,\ h_2 = 1\ m,\ \rho = 1\ kg/m,\ x_{c0} = 0\ m,\ x_{w0} = 190\ m.$

The system model is simulated by MATLAB program and solved by Runge–Kutta method with the above parameters.

4.1. Design the minimum IAEE for a 7-R profile

The SLPSO method is applied to search for the optimal σ value in association with minimizing the F_f. The numerical simulation parameters are employed and the numerical results are shown in Fig. 4. Fig. 4(a) shows that the fraction σ is searched rapidly and $\sigma = 0.5$ is the optimal value finally. Similarly, Fig. 4(b) shows the F_f with the searched σ and the final value of the fitness function is $F_f = 41210.43J$ after 3 iterations. It can be found that the minimum IAEE profile has a non-maximum acceleration region.

To compare the profiles with different σ values, $\sigma = 0.1$, $\sigma = 0.2$ and $\sigma = 0.5$ are compared and the trajectories, input voltages and currents are also compared in Fig. 5. It is found that the trajectories with $\sigma = 0.1$ and $\sigma = 0.2$ has a short

Please cite this article as: K.-Y. Chen, R.-F. Fung, The point-to-point multi-region energy-saving trajectory planning for a mechatronic elevator system, Applied Mathematical Modelling (2016), http://dx.doi.org/10.1016/j.apm.2016.06.001

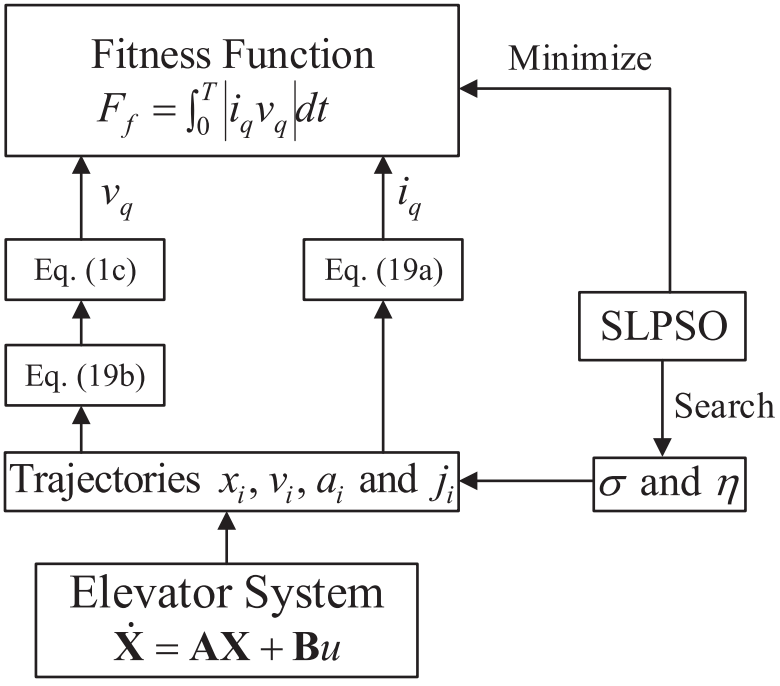

Fig. 3. The process of energy saving trajectory planning by SLPSO method.

Table 1
Comparisons of different fractions σ in the input energy and flight time for a 7-R profile.

	$\sigma = 0.1$	$\sigma = 0.2$	$\sigma = 0.5$
$E_i(J)$	53,883.97 (α_1)	51,903.76 (α_2)	41,210.43 (α_3)
Flight time t_7 (s)	37.41 (β_1)	38.33 (β_2)	43.33 (β_3)
Input energy relative error (%)	–	$\frac{\alpha_2-\alpha_1}{\alpha_1} \times 100\% = -3.67\%$	$\frac{\alpha_3-\alpha_1}{\alpha_1} \times 100\% = -23.52\%$
Flight time relative error (%)	–	$\frac{\beta_2-\beta_1}{\beta_1} \times 100\% = 2.46\%$	$\frac{\beta_3-\beta_1}{\beta_1} \times 100\% = 15.82\%$

flight time and the trajectory with $\sigma = 0.5$ has the longest flight time. In Fig. 5(c) and (d), it is found that the trajectory with $\sigma = 0.5$ has a non-maximum acceleration region and has small jerk responses. The input voltages and currents have the similar responses with acceleration responses, which are compared in Fig. 5(e) and (f).

The input electrical energy E_i, the dissipation energy E_d, the magnetic energy E_m and the kinetic energy E_k with $\sigma = 0.1$, $\sigma = 0.2$ and $\sigma = 0.5$ are compared in Fig. 6. In Fig. 6(a) and (b), it is found that the trajectories with $\sigma = 0.1$ and $\sigma = 0.2$ have large E_i and E_d, the trajectory with $\sigma = 0.5$ has small E_i and E_d. It can be concluded that the acceleration response is the major energy consumption region, which is caused by the dissipation energy E_d. In Fig. 6(c) and (d), the magnetic and kinetic energies are all from null to null. It can be concluded that trajectories with $\sigma = 0.1$ and $\sigma = 0.2$ have the short flight time but large IAEE. The trajectory with $\sigma = 0.5$ has the longest flight time but the smallest IAEE. Finally, the comparisons among trajectories with $\sigma = 0.1$, $\sigma = 0.2$ and $\sigma = 0.5$ in input electrical energy and the final time are described in Table 1. It is found that trajectory with $\sigma = 0.5$ can save 23.52% input electrical energy but spend 15.82 % flight time. Trajectory with $\sigma = 0.2$ can save 3.67% input energy but spend 2.46 % flight time. The above percentage values are compared with respective to that of $\sigma = 0.1$. It can be concluded that both the input electrical energy and flight time are simultaneously contradictory in the trajectory planning.

4.2. Design the minimum IAEE for a 3-R profile

The SLPSO method is also applied to search for the optimal η value in associate with minimizing the F_f for a 3-R profile. The parameters are the same with those in Section 4.1. Fig. 7 shows the optimal value η and fitness function by the SLPSO. It is found that the optimal value η is 0.4 by the SLPSO, the fitness function has the minimum value ($F_f = 41693.15$). To prove the optimal value ($\eta = 0.4$) can find the minimum IAEE, $\eta = 0.5$ is chosen to compare in Fig. 8, where the trajectory responses, input electrical voltages and currents are compared between $\eta = 0.4$ and $\eta = 0.5$. It is found that the difference is

Please cite this article as: K.-Y. Chen, R.-F. Fung, The point-to-point multi-region energy-saving trajectory planning for a mechatronic elevator system, Applied Mathematical Modelling (2016), http://dx.doi.org/10.1016/j.apm.2016.06.001

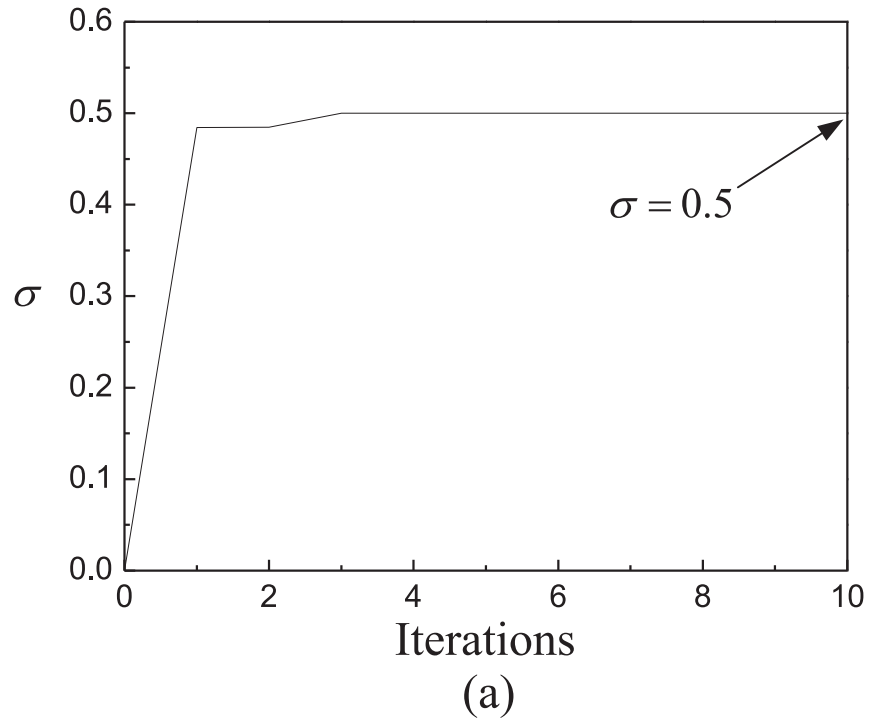

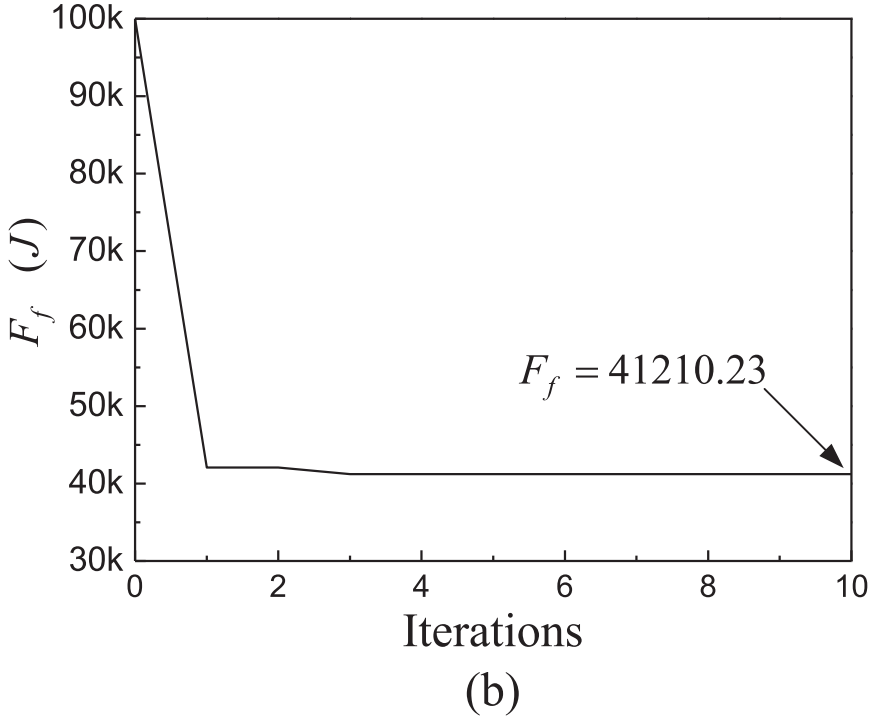

Fig. 4. Optimal value σ and fitness value by the SLPSO for a 7-R profile.

small, the flight times of $\eta = 0.4$ is 41.85 s and $\eta = 0.5$ is 42.5 s. The comparisons of input, dissipation, magnetic and kinetic energies are shown in Fig. 9. It is found that input energy with $\eta = 0.4$ is less than $\eta = 0.5$ in Fig. 9(a). Dissipation energy also has the same results with input electrical energy as shown in Fig. 9(b). Magnetic and kinetic energies all converge into null at the final time as shown in Fig. 9(c) and (d), respectively. The details of Fig. 9 are illustrated in Table 2. It can be observed that the 3-R profile with $\eta = 0.4$ has less input energy and flight time than the trajectory with $\eta = 0.5$.

Please cite this article as: K.-Y. Chen, R.-F. Fung, The point-to-point multi-region energy-saving trajectory planning for a mechatronic elevator system, Applied Mathematical Modelling (2016), http://dx.doi.org/10.1016/j.apm.2016.06.001

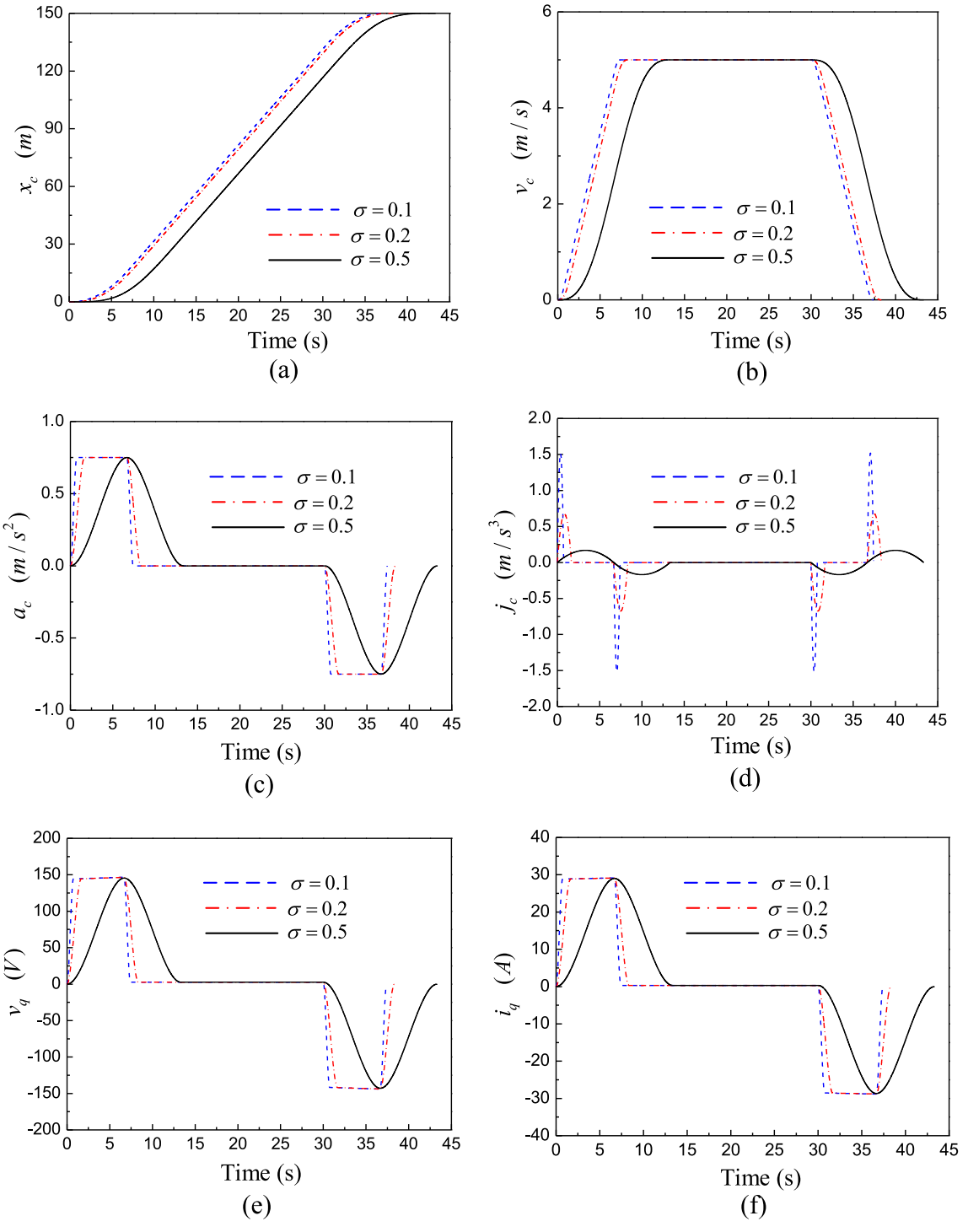

Fig. 5. Comparisons of trajectory responses among $\sigma = 0.1$, $\sigma = 0.2$ and $\sigma = 0.5$ for a 7-R profile.

Table 2
Comparisons of fractions η in the input energy and flight time for a 3-R profile.

	$\eta = 0.4$	$\eta = 0.5$
$E_i(J)$	41,693.15	42,266.58
Flight time τ_3 (s)	41.85	42.50

Please cite this article as: K.-Y. Chen, R.-F. Fung, The point-to-point multi-region energy-saving trajectory planning for a mechatronic elevator system, Applied Mathematical Modelling (2016), http://dx.doi.org/10.1016/j.apm.2016.06.001

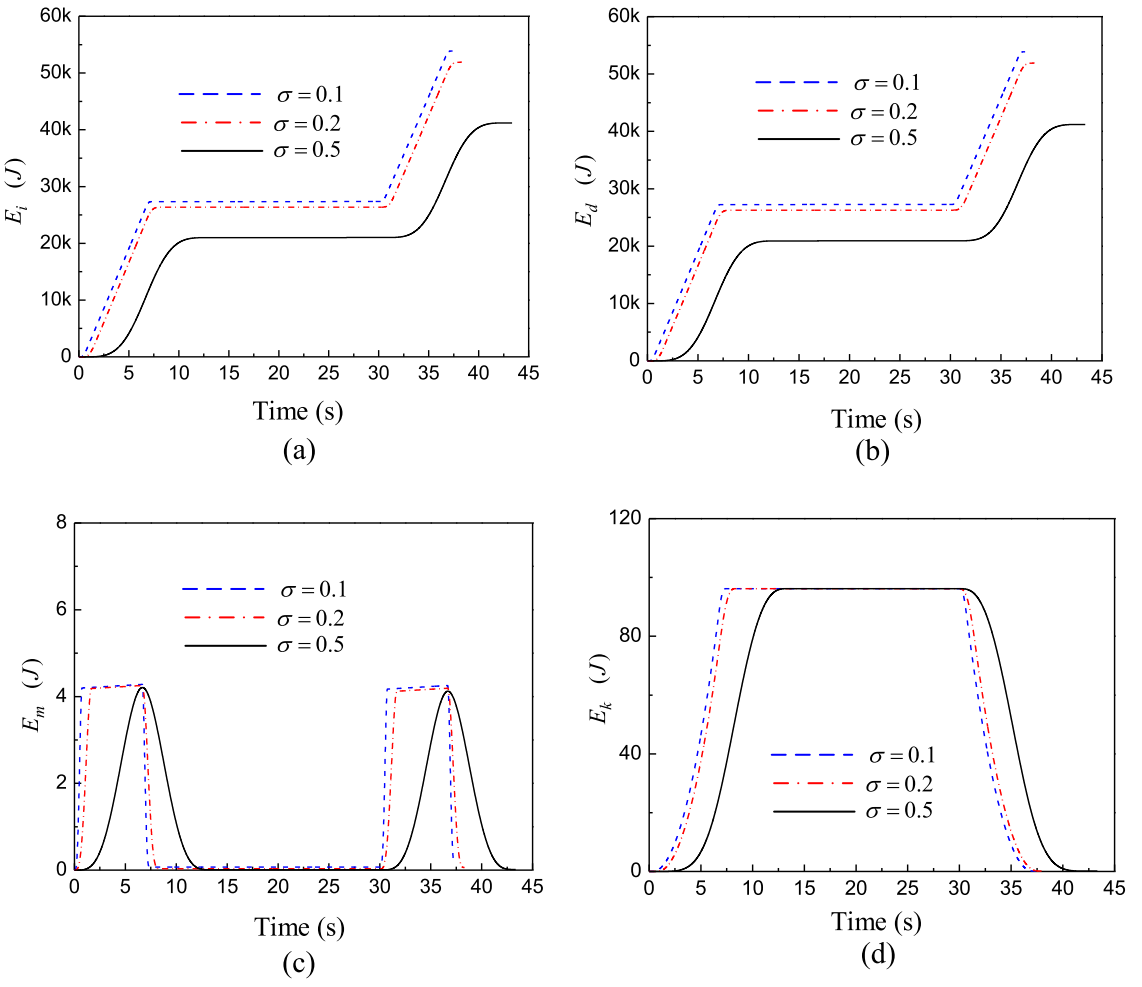

Fig. 6. Comparisons among E_i, E_d, E_m and E_k with $\sigma = 0.1$, $\sigma = 0.2$ and $\sigma = 0.5$ for a 7-R profile.

Table 3
Comparisons between the 7-R and 3-R profiles with system parameters, groups 1 and 2.

Profile	System parameters	Fraction	IAEE	Remark
7-R profile	Group 1	$\sigma = 0.5$	41,210.43	Minimum
		$\sigma = 0.4$	45,963.08	
	Group 2	$\sigma = 0.5$	6205.43	Minimum
		$\sigma = 0.4$	6921.03	
3-R profile	Group 1	$\eta = 0.4$	41,693.15	Minimum
		$\eta = 0.5$	42,266.58	
	Group 2	$\eta = 0.4$	6278.14	Minimum
		$\eta = 0.5$	6364.45	

4.3. Comparisons between the 7-R and 3-R profiles with new system parameters

In Sections 4.1 and 4.2, the 7-R profile with $\sigma = 0.5$ and 3-R profile with $\eta = 0.4$ have the minimum IAEE by using the numerical parameters (Group 1). In this section, to confirm they also have the minimum IAEE, new system parameters (Group 2) are performed and shown as follows:

$J_m = 1 \times 10^{-3}\ kgm^2,\ B_m = 5 \times 10^{-3}\ Nms/rad,\ K_t = 8\ Nm/A,\ R_s = 10\ \Omega,\ \lambda_d = 0.01\ N - s/rad,$
$L_q = 0.05\ H,\ J = 0.1\ kgm^2,\ R = 0.25\ m,\ m_c = 80\ kg,\ m_w = 50\ kg,\ c = 0.6\ Ns/m,\ n = 1,$
$H = 200\ m,\ h_0 = 2\ m,\ h_1 = 1\ m,\ h_2 = 1\ m,\ \rho = 1\ kg/m,\ x_{c0} = 0m$ and $x_{w0} = 190\ m.$

Their comparison between the 7-R and 3-R profiles with parameter groups 1 and 2 is illustrated in Table 3. It is found that the 7-R profile with $\sigma = 0.5$ and 3-R profile with $\eta = 0.4$ also have the minimum IAEE for the same elevator model.

Please cite this article as: K.-Y. Chen, R.-F. Fung, The point-to-point multi-region energy-saving trajectory planning for a mechatronic elevator system, Applied Mathematical Modelling (2016), http://dx.doi.org/10.1016/j.apm.2016.06.001

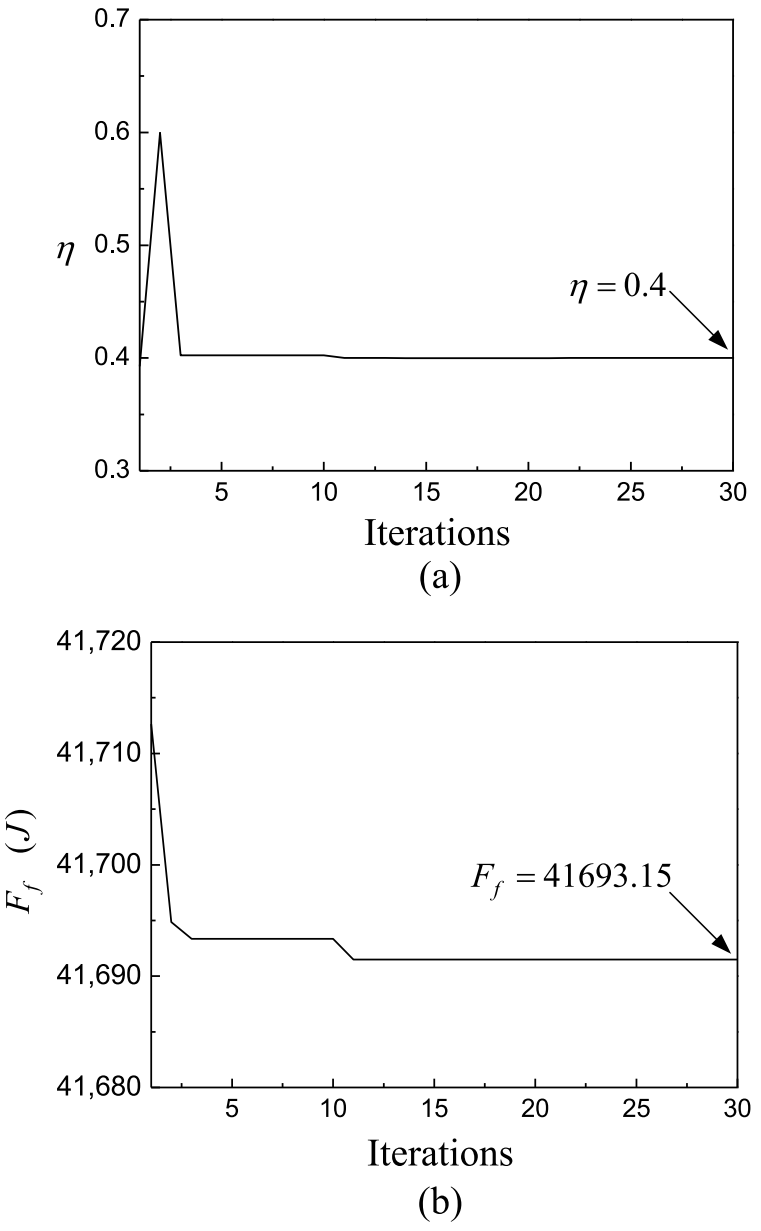

Fig. 7. Optimal value η and fitness values by the SLPSO for a 3-R profile.

4.4. Discussion and summary

According to the above simulation results, it is found that $\sigma = 0.5$ can obtain the minimum IAEE for a 7-R profile. Therefore, the 7-R profile can be substituted by a 5-R profile with $\sigma = 0.5$. It is shown in Fig. 10 and each region (region $1' \sim$ region $5'$) is described as follows:

(1) region $1'$

$$x(t) = k_{10} + k_{11}(t - t_0) + k_{12}(t - t_0)^2 + k_{13}(t - t_0)^3 + k_{14}(t - t_0)^4 + k_{15}(t - t_0)^5, \tag{17a}$$

$$v(t) = k_{11} + 2k_{12}(t - t_0) + 3k_{13}(t - t_0)^2 + 4k_{14}(t - t_0)^3 + 5k_{15}(t - t_0)^4, \tag{17b}$$

$$a(t) = 2k_{12} + 6k_{13}(t - t_0) + 12k_{14}(t - t_0)^2 + 20k_{15}(t - t_0)^3, \tag{17c}$$

$$j(t) = 6k_{13} + 24k_{14}(t - t_0) + 60k_{15}(t - t_0)^2. \tag{17d}$$

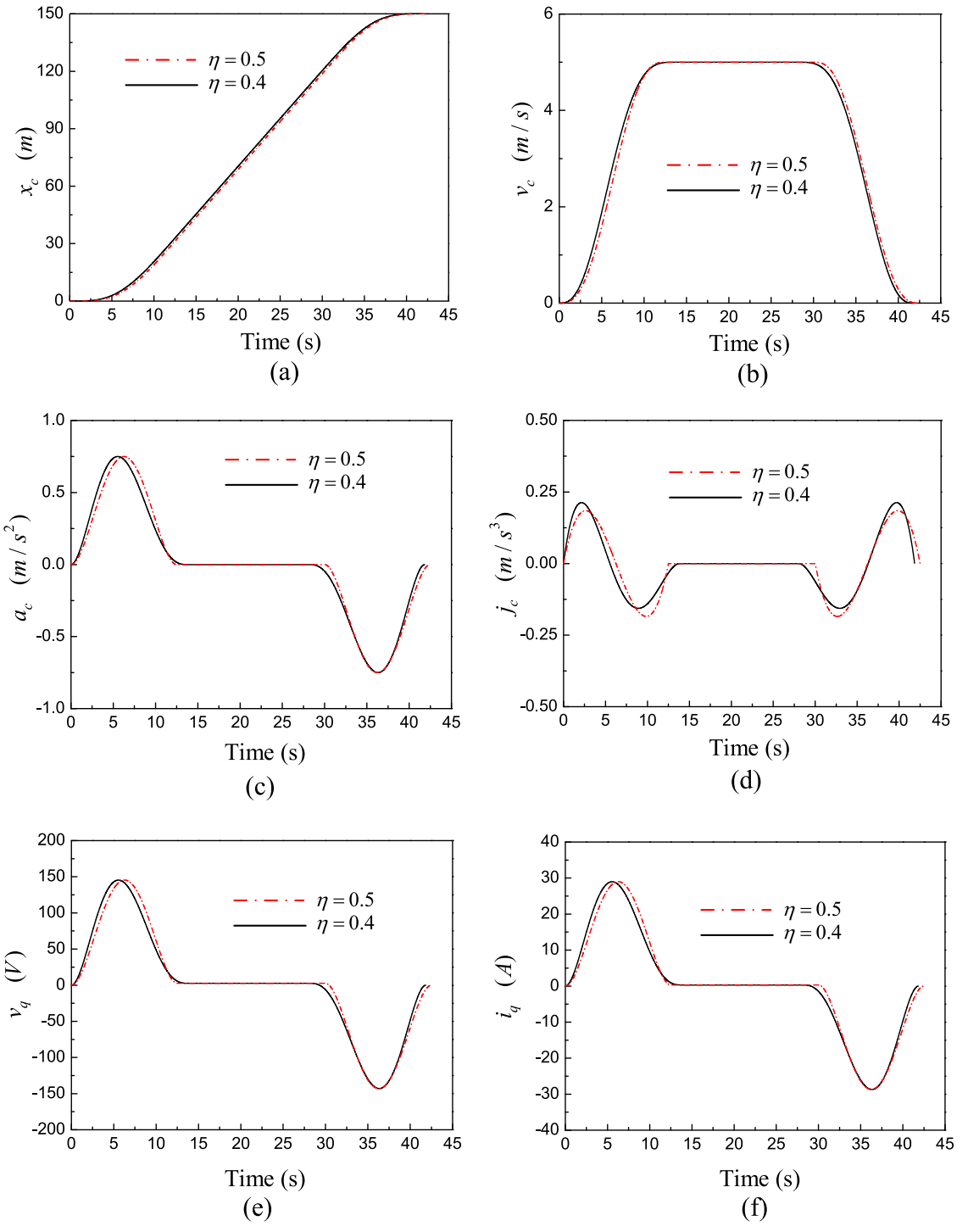

Fig. 8. Comparisons of trajectory responses between $\eta = 0.4$ and $\eta = 0.5$ for a 3-R profile.

where $k_{10} = k_{11} = k_{12} = k_{13} = 0$, $k_{14} = a_{\max}/(t_{2'} - t_0)^2$, $k_{15} = -4a_{\max}/5(t_{2'} - t_0)^3$, $t_{2'} = 2v_{\max}/a_{\max}$ and $t_{1'} = v_{\max}/a_{\max}$.

(2) region 2′

$$x(t) = k_{20} + k_{21}(t - t_{1'}) + k_{32}(t - t_{1'})^2 + k_{33}(t - t_{1'})^3 + k_{34}(t - t_{1'})^4 + k_{35}(t - t_{1'})^5, \tag{18a}$$

$$v(t) = k_{21} + 2k_{22}(t - t_{1'}) + 3k_{23}(t - t_{1'})^2 + 4k_{24}(t - t_{1'})^3 + 5k_{25}(t - t_{1'})^4, \tag{18b}$$

Please cite this article as: K.-Y. Chen, R.-F. Fung, The point-to-point multi-region energy-saving trajectory planning for a mechatronic elevator system, Applied Mathematical Modelling (2016), http://dx.doi.org/10.1016/j.apm.2016.06.001

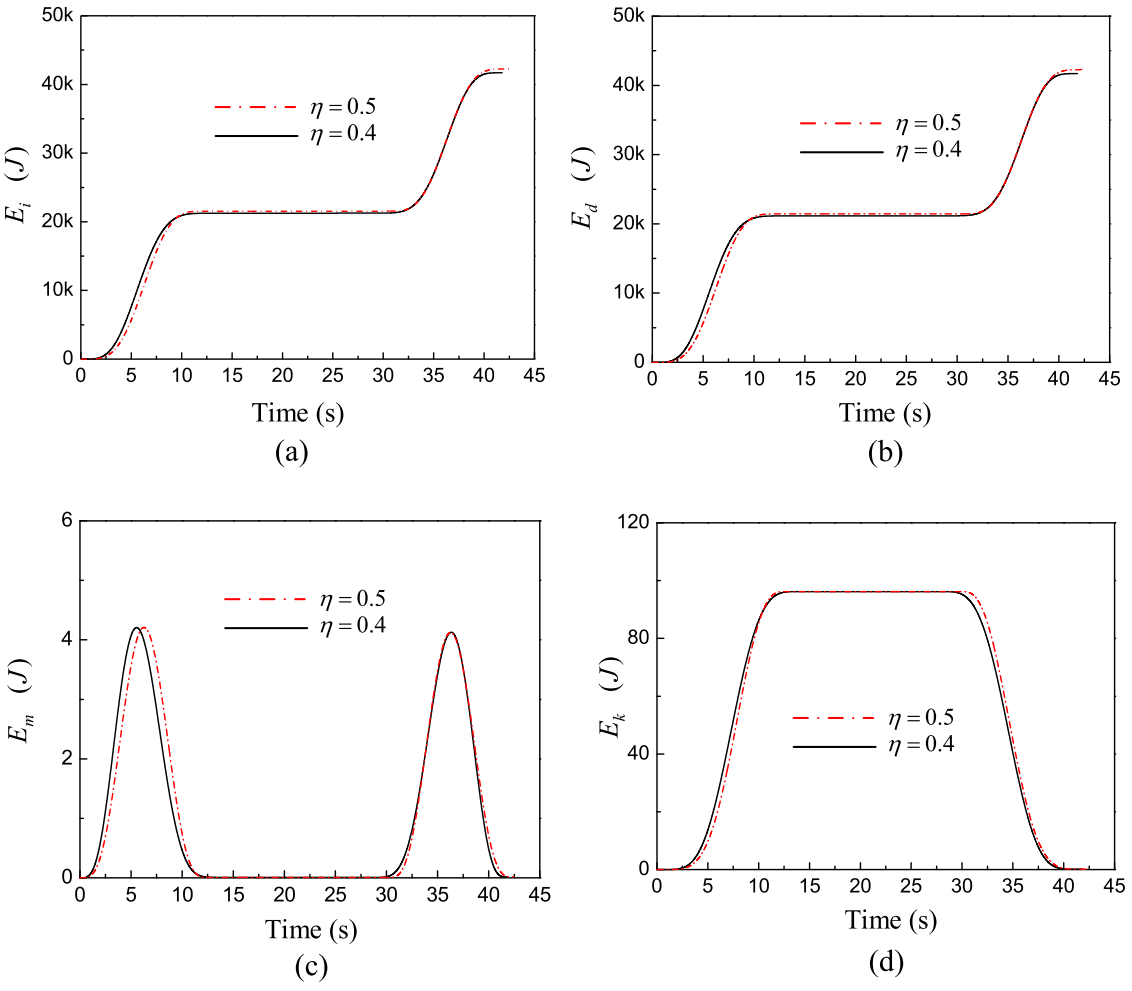

Fig. 9. Comparisons among E_i, E_d, E_m and E_k with $\eta = 0.4$ and $\eta = 0.5$ for a 3-R profile.

$$a(t) = 2k_{22} + 6k_{23}(t - t_{1'}) + 12k_{24}(t - t_{1'})^2 + 20k_{25}(t - t_{1'})^3, \tag{18c}$$

$$j(t) = 6k_{23} + 24k_{24}(t - t_{1'}) + 60k_{25}(t - t_{1'})^2. \tag{18d}$$

where $k_{20} = x(t_{1'})$, $k_{21} = v(t_{1'})$, $k_{22} = a_{\max}/2$, $k_{23} = 0$,$k_{24} = -k_{14} = -a_{\max}/(t_{2'} - t_0)^2$, $k_{25} = -k_{15} = 4a_{\max}/5(t_{2'} - t_0)^3$.

(3) region 3′

$$x(t) = k_{30} + k_{31}(t - t_{2'}), \tag{19a}$$

$$v(t) = v_{\max}, \tag{19b}$$

$$a(t) = 0, \tag{19c}$$

$$j(t) = 0. \tag{19d}$$

where $k_{30} = x(t_{2'})$, $k_{31} = v_{\max}$ and $t_{3'} = t_{2'} + \frac{h - 2x(t_{2'})}{v_{\max}}$.

(4) region 4′

$$x(t) = x(t_{3'}) + v_{\max}(t - t_{3'}) + k_{44}(t - t_{3'})^4 + k_{45}(t - t_{3'})^5, \tag{20a}$$

$$v(t) = v_{\max} + 4k_{44}(t - t_{3'})^3 + 5k_{45}(t - t_{3'})^4, \tag{20b}$$

$$a(t) = 12k_{44}(t - t_{3'})^2 + 20k_{45}(t - t_{3'})^3, \tag{20c}$$

Please cite this article as: K.-Y. Chen, R.-F. Fung, The point-to-point multi-region energy-saving trajectory planning for a mechatronic elevator system, Applied Mathematical Modelling (2016), http://dx.doi.org/10.1016/j.apm.2016.06.001

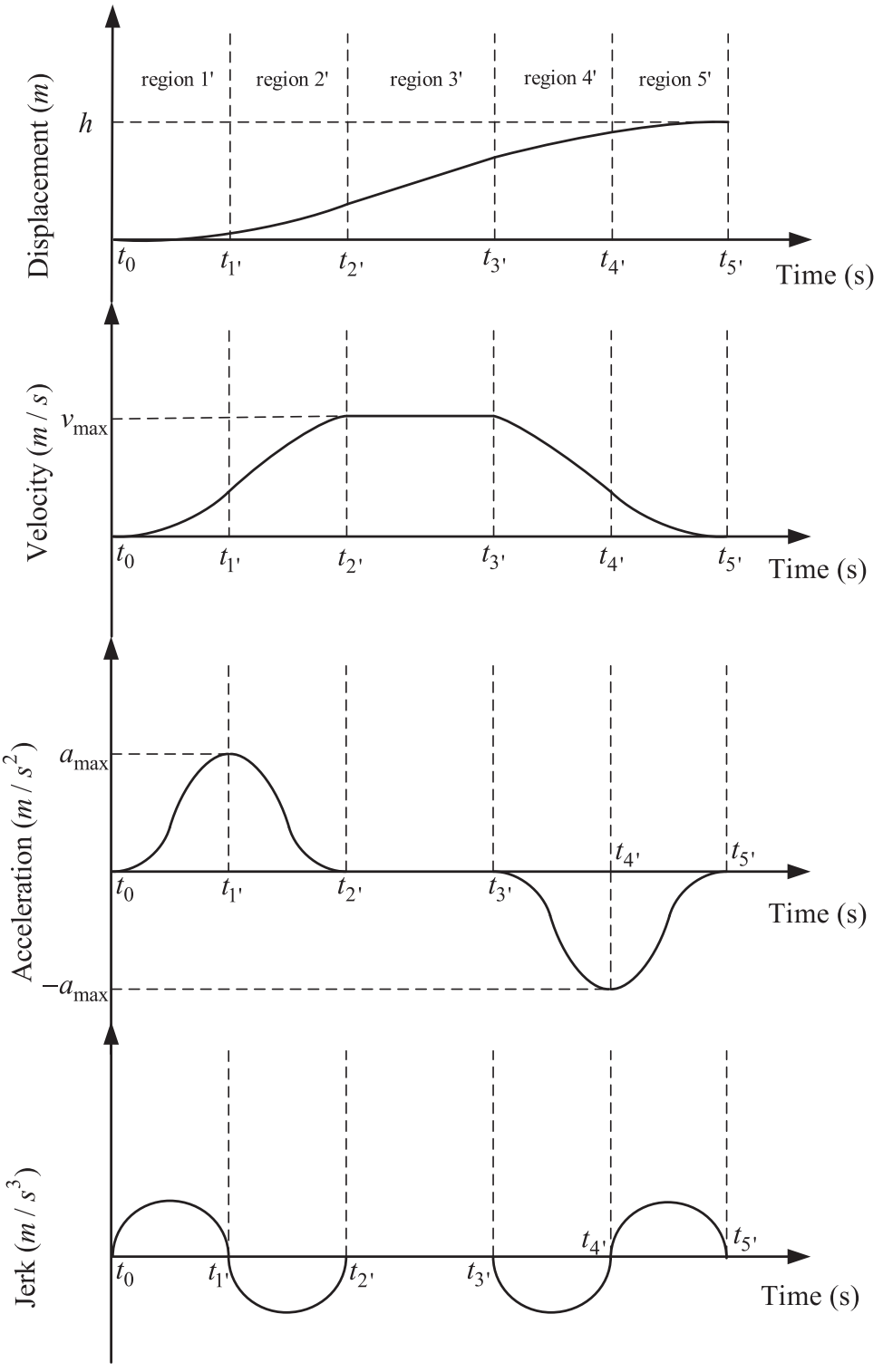

Fig. 10. The new 5-R profile with $t_{1'} - t_0 = t_{2'} - t_{1'} = t_{4'} - t_{3'} = t_{5'} - t_{4'}$.

Please cite this article as: K.-Y. Chen, R.-F. Fung, The point-to-point multi-region energy-saving trajectory planning for a mechatronic elevator system, Applied Mathematical Modelling (2016), http://dx.doi.org/10.1016/j.apm.2016.06.001

$$j(t) = 24k_{44}(t - t_{3'}) + 60k_{45}(t - t_{3'})^2. \tag{20d}$$

where $k_{44} = -k_{14} = -a_{\max}/(t_{2'} - t_0)^2$, $k_{45} = -k_{15} = 4a_{\max}/5(t_{2'} - t_0)^3$ and $t_{4'} = t_{3'} + t_{2'}/2$.

(5) region 5′

$$x(t) = k_{50} + k_{51}(t - t_{4'}) + k_{52}(t - t_{4'})^2 + k_{53}(t - t_{4'})^3 + k_{54}(t - t_{4'})^4 + k_{55}(t - t_{4'})^5, \tag{21a}$$

$$v(t) = k_{51} + 2k_{52}(t - t_{4'}) + 3k_{53}(t - t_{4'})^2 + 4k_{54}(t - t_{4'})^3 + 5k_{55}(t - t_{4'})^4, \tag{21b}$$

$$a(t) = 2k_{52} + 6k_{53}(t - t_{4'}) + 12k_{54}(t - t_{4'})^2 + 20k_{55}(t - t_{4'})^3, \tag{21c}$$

$$j(t) = 6k_{53} + 24k_{54}(t - t_{4'}) + 60k_{55}(t - t_{4'})^2. \tag{21d}$$

where $k_{50} = x(t_{4'}), k_{51} = v(t_{4'})$, $k_{52} = -a_{\max}/2, k_{53} = 0,$, $k_{54} = a_{\max}/(t_{2'} - t_0)^2$, $k_{55} = -4a_{\max}/5(t_{2'} - t_0)^3$ and $t_{5'} = t_{3'} + t_{2'}$.

From the numerical simulations in Section 4.1, it is found that trajectory with $\sigma = 0.5$ has the minimum IAEE, but the longest flight time. It means that the less time of maximum acceleration is performed, the less IAEE is consumed. Observing the dissipation energy E_d, large velocity produces large dissipation energy. Similarly, large acceleration produces large velocity and dissipation energy. It can be concluded that the acceleration and deceleration are the major energy consumption for the mechatronic system.

To simplify the design of a 7-R profile, the 3-R profile is proposed and can be described by a 7-D polynomial with the same boundary constraint conditions. The fraction η can also be adjusted by the SLPSO with minimizing the IAEE. From the numerical simulations, it is found that the optimal fraction $\eta = 0.4$ can obtain the minimum IAEE and the shortest flight time when compared with $\eta = 0.5$. Comparing between Tables 1 and 2, the 7-R profile with $\sigma = 0.5$ has less IAEE than the 3-R profile with $\eta = 0.4$. The relative error of the IAEE is 1.171%. But a 3-R profile with $\eta = 0.4$ has less flight time than the 7-R profile with $\sigma = 0.5$. The relative error of flight time is 3.536%. Finally, the 7-R profile is modified as a 5-R profile with $\sigma = 0.5$ by the SLPSO with the minimum IAEE for the mechatronic elevator system. Furthermore, to simplify the design of a 5-R profile with the same constraint conditions, the 3-R profile is proposed by a 7-D polynomial trajectory with the minimum IAEE. Their relative errors of the IAEE and flight time are small.

5. Conclusions

The mechatronic elevator system driven by a PMSM is mathematically modeled, and the energy equations in the electrical and mechanical parts are also formulated. The 7-R profile is discussed and the optimal fraction $\sigma = 0.5$ has been obtained with minimizing the IAEE by the SLPSO method. In other words, trajectory with $\sigma = 0.5$ has the non-maximum acceleration (deceleration) region, the minimum IAEE and longest flight time. On the contrary, the simple 3-R profile is proposed by a 7-D polynomial trajectory with the same constraint conditions. The optimal fraction $\eta = 0.4$ is found by the SLPSO with the minimum IAEE. Specially, the different parameters, groups 1 and 2, are compared, and it is found the 7-R profile with $\sigma = 0.5$ and 3-R profile with $\eta = 0.4$ also have the minimum IAEE for the same system model. It means that the optimal solutions are insensitive to the system model. Finally, the new 5-R and 3-R profiles are compared and their relative errors of the IAEE and flight time are small. In summary, when the final position, maximum velocity and acceleration are specified for any mechatronic system, the proposed trajectory design method can also be applied for a PTP multi-region profile with the minimum IAEE.

Acknowledgment

The authors are grateful to the Ministry of Science and Technology for the finical support under contract no. MOST 103-2221-E-327-009 -MY3.

References

[1] A. Khoukhi, L. Baron, M. Balazinski, K. Demirli, A hierarchical neuro-fuzzy system to near optimal-time trajectory planning of redundant manipulators, Eng. Appl. Artif. Intell. 21 (2008) 974–984.
[2] L. Biagiotti, C. Melchiorri, FIR filters for online trajectory planning with time- and frequency-domain specifications, Control Eng. Pract. 20 (12) (2012) 1385–1399.
[3] Q. Zhang, S. Li, J. Guo, Smooth time-optimal tool trajectory generation for CNC manufacturing systems, J. Manuf. Syst. 31 (2012) 280–287.
[4] H. Liu, X. Lai, W. Wu, Time-optimal and jerk-continuous trajectory planning for robot manipulators with kinematic constraints, Rob. Comput. Integr. Manuf. 29 (2013) 309–317.
[5] Y. Zhuang, H. Huang, Time-optimal trajectory planning for underactuated spacecraft using a hybrid particle swarm optimization algorithm, Acta Astronaut. 94 (2014) 690–698.
[6] P. Lambrechts, M. Boerlage, M. Steinbuch, Trajectory planning and feedforward design for electromechanical motion systems, Control Eng. Pract. 13 (2005) 145–157.
[7] A. Gasparetto, V. Zanotto, A new method for smooth trajectory planning of robot manipulators, Mech. Mach. Theory 42 (2007) 455–471.
[8] X. Wang, J. Wang, Z. Rao, An adaptive parametric interpolator for trajectory planning, Adv. Eng. Software 41 (2010) 180–187.
[9] M. Reza Azizi, D. Naderi, Dynamic modeling and trajectory planning for a mobile spherical robot with a 3Dof inner mechanism, Mech. Mach. Theory 64 (2013) 251–261.

Please cite this article as: K.-Y. Chen, R.-F. Fung, The point-to-point multi-region energy-saving trajectory planning for a mechatronic elevator system, Applied Mathematical Modelling (2016), http://dx.doi.org/10.1016/j.apm.2016.06.001

[10] B. Su, L. Zou, Manipulator trajectory planning based on the algebraic-trigonometric hermite blended interpolation spline, Procedia Eng. 29 (2012) 2093–2097.
[11] P. Boscariol, A. Gasparetto, Model-based trajectory planning for flexible-link mechanisms with bounded jerk, Rob. Comput. Integr. Manuf. 29 (2013) 90–99.
[12] C. Zheng, Y. Su, P.C. Muller, Simple online smooth trajectory generations for industrial systems, Mechatronics 19 (2009) 571–576.
[13] A. Abe, Trajectory planning for residual vibration suppression of a two-link rigid-flexible manipulator considering large deformation, Mech. Mach. Theory 44 (2009) 1627–1639.
[14] A. Trevisani, Underconstrained planar cable-direct-driven robots: A trajectory planning method ensuring positive and bounded cable tensions, Mechatronics 20 (2010) 113–127.
[15] Y. Wang, K. Ueda, S.A. Bortoff, A Hamiltonian approach to compute an energy efficient trajectory for a servomotor system, Automatica 49 (12) (2013) 3550–3561.
[16] C.T. Chen, T.T. Liao, A hybrid strategy for the time- and energy-efficient trajectory planning of parallel platform manipulators, Rob. Comput. Integr. Manuf. 27 (2011) 72–81.
[17] Y. Hsu, M.S. Huang, R.F. Fung, Energy-saving trajectory planning for a toggle mechanism driven by a PMSM, Mechatronics 24 (2014) 23–31.
[18] R.F. Fung, Y.H. Cheng, Trajectory planning based on minimum absolute input energy for an LCD glass-handling robot, Appl. Math. Modell. 38 (2014) 2837–2847.
[19] M.S. Huang, Y.L. Hsu, R.F. Fung, Minimum-energy point-to-point trajectory planning for a motor-toggle servomechanism, IEEE/ASME Trans. Mechatron. 17 (2) (2012).
[20] W.D. Zhu, L.J. Teppo, Design and analysis of a scaled model of a high-rise, high-speed elevator, J. Sound Vib. 264 (2003) 707–731.
[21] K.Y. Chen, M.S. Huang, R.F. Fung, Adaptive minimum-energy tracking control for the mechatronic elevator system, IEEE Trans. Control Syst. Technol. (99) (2013) 1–10.
[22] C. Li, S. Yang, T.T. Nguyen, A self-learning particle swarm optimizer for global optimization problems, IEEE Trans. Syst. Man. Cybern. Part B Cybern. 42 (3) (2012) 627–646.
[23] K.Y. Chen, M.S. Huang, R.F. Fung, Dynamic modelling and input-energy comparison for the elevator system, Appl. Math. Modell. 38 (2014) 2037–2050.
[24] J. Kennedy, R. Eberhart, Particle swarm optimization, Proc. IEEE Int. Conf. Neural Netw (ICNN) 4 (1995) 1942–1948.
[25] R. Eberhart, J. Kennedy, A new optimizer using particle swarm theory, in: Proceedings of the 6th International Symposium on Micro Machine and Human Science (MHS). Oct, 1995, pp. 39–43.

Please cite this article as: K.-Y. Chen, R.-F. Fung, The point-to-point multi-region energy-saving trajectory planning for a mechatronic elevator system, Applied Mathematical Modelling (2016), http://dx.doi.org/10.1016/j.apm.2016.06.001